High-speed driving of Lateral Guided Robotic Vehicle with a Rear Wheel Steer Mechanism Controlled by SSM

Yoshihiro Takita, Hisashi Date and Shinya Ohkawa

Abstract—**This paper proposes SSM(Sensor Steering Mechanism) for lateral guided vehicle with rear wheel steering mechanism. Authors demonstrated the geometry of SSM for the front wheel steer type and the reverse phase four-wheel steer type one. SSM presents a stable lateral guiding performance for automated vehicle which follows a straight and curved path created by guideway. The other hand, SSM is not established for a rear wheel steer type vehicle. Rear wheel steer vehicles are forklifts and backward moving of the conventional motor vehicles of which steering wheels are located at the front. SSM for the rear wheel steer vehicles enables a forklift to automated moving on every spaces, if the control method by SSM is established. This paper leads SSM relation for a rear wheel steer vehicle and constructs an experimental robotic vehicle with proposed SSM. Simulated and experimental data show the advantages of proposed SSM.**

Index Terms—**Lateral guided, SSM, Rear wheel steer, Robotic Vehicle**

I. INTRODUCTION

NOT only automated factories but also many other fields are used AGVs (Automated Guided Vehicle)for the productive efficiency and the labor cost saving. The problem is the moving stability of the vehicle in the lateral direction resulting from dynamical characteristics by the sensor position and controlling mechanism. A practical speed limit of the AGV[1-4] used in manufacturing factory is approximately 2m/s. On the other hand, the DMT (Dual Mode Truck)[5], which has been investigated in recent years, is driven by a human operator on ordinary roads, and is controlled automatically on roads added mechanical guidance devices. However, the speed limit for the stable tracking is existing due to the geometry of guiding mechanism. In 2005 through 2007, the DARPA (Defense Advanced Research Projects Agency)[6] held the grand challenge which spurred many robotics researchers to develop the autonomous vehicle first. The average speed of the top vehicle was about 30 km/h. As it is still a long way off the human driving technique, many technical problems have appeared from this competition. In the case of following the center line of the road, the important thing is that how to control the steering angle without lateral instability. The authors proposed a SSM (Sensor Steering Mechanism) for a laterally guided vehicle with front[7] and four-wheel steering mechanism[8]. When the vehicle is guided by the SSM, it has been shown that no speed limit exists on the straightline travel, except with respect to the over steer characteristics. In addition,

Yoshihiro Takita: Department of Computer Science, National Defense Academy, Japan (e-mail: takita@nda.ac.jp)
Hisashi Date:(e-mail: date@nda.ac.jp)
Shinya Ohkawa:(e-mail: em50045@nda.ac.jp)

the experimental results obtained using a newly developed robotic vehicle revealed that the SSM follows the guideway while adjusting the centrifugal force and the sideforce of the tires when traveling around corners. Furthermore, the previous paper derived the dynamic equations of motion and calculated the movement of the controlled vehicle by SSM along with the experimentally measured tire characteristics. For the accuracy simulation of vehicle moving at high speed, the authors proposed the variable kinetic friction model of the tire and applied it to the derived dynamical equations[9]. The existence of the sensor arm prevents the application of SSM to the vehicle operating on ordinary road. In the last paper it was solved by replacing the sensor arm with a miniaturized 1kHz intelligent camera[10-12]. This paper paid attention to the forklift which is widely used for the cargo handling operation, but the SSM is not applied to this type vehicle of which steering mechanism is located at the rear. The other hand when the car runs to back, it can be considered the rear wheel steering vehicle. If the SSM can be applied, the speed-up of lateral guided vehicle with rear steer mechanism is able to be expected. This paper proposed a SSM for the rear steering vehicle, and the ratio of steering angle and sensor arm angle is desired. An experimental set up is developed and tested on the test course. A dynamical model of experimental vehicle is derived, and applied the variable kinetic friction model for tire model to simulate a moving trajectory. Experimental results of high-speed movement and the moving simulation are presented. These results demonstrate that the SSM for rear steering vehicle can perform at high-speed movement and maintain stability on the course.

II. SSM AND DYNAMICAL MODEL

A. Sensor Steering Mechanism(SSM)

Figure 1 shows a schematic idea of SSM for a lateral guided vehicle with rear wheel steering mechanism by the bicycle model. SSM shows the mechanical relation when the vehicle moves in steady state. It is necessary to verify whether this idea is effective for high-speed moving on a test course by the experiment and simulation. A front steer type SSM and proposed rear steer type SSM are shown in Fig. 1. It is assumed that backward moving of a front steer vehicle is a rear steer vehicle. The front steer type SSM and rear steer type SSM are consisted with PQS_f and QPS_r, respectively. When the rear steer type vehicle moves counterclockwise on radius R by the steering angle δ , then a front tire A moves on the radius R but a rear tire Q moves outside of the course. Here, S_f is a sensor of the front steer type SSM,

and it follows giudeway correctly. Then the angle of sensor arm QS_f is 2δ. A triangle PQO and PEO are a congruous each other, and it is assumed to be S_r that the circular arc intersects with segment EO. The relation between the sensor arm angle ϕ and steering angle δ is as follows;

$$\delta = 2\phi \quad (1)$$

The sensor arm length PS_r is

$$\overline{PSr} = 2R\sin\delta/2 \quad (2)$$

A linearized equation at the equilibrium point is obtained as follow;

$$\overline{PSr} = R\delta \approx L \quad (3)$$

B. Dynamical Equation of Motion

Figure 2 shows the rigid body bicycle vehicle model moving at V. It is assumed that the right and left tires have same characteristics. In figure 2, N is the Newton reference frame. Dextral sets of mutually perpendicular unit vectors $\boldsymbol{n}_1$ and $\boldsymbol{n}_2$ are fixed in N. The reference frame A is fixed on the vehicle, and the mutually perpendicular unit vectors $\boldsymbol{a}_1$ and $\boldsymbol{a}_2$ are fixed in A. Here, θ is the body position angle, γ is the yaw angle, δ_f and δ_r are the steering angles of the front and rear tires, respectively, β_f and β_r are the slip angles of the front and rear tires, respectively. γ_f and γ_r are the angles between $\boldsymbol{n}_1$ and the velocity vector of the front and rear axles, respectively. In addition, U_f and U_r are the cornering forces of the front and rear tires, respectively. l_f and l_r are the distances from the center of gravity to the front and rear axles, respectively. m is the mass, and I is the moment of inertia about the yaw-axis of the vehicle. Finally, F_f and F_r are the driving forces, and D_f and D_r are the rolling resistance forces of the front and rear tires, respectively. The dynamic equations of motion are derived as follows:

$$
\begin{aligned}
mx =\ & -F_f\cos(\theta+\delta_f) - U_f\sin(\theta+\delta_f)\\
& -U_r\sin(\theta+\delta_r) - F_r\cos(\theta+\delta_r)\\
& -D_r(l_r\dot{\theta}\sin\theta + D_r\dot{x})/E.
\end{aligned} \quad (4)
$$

$$
\begin{aligned}
my =\ & F_f\sin(\theta+\delta_f) + U_f\cos(\theta+\delta_f)\\
& +U_r\cos(\theta+\delta_r) + F_r\sin(\theta+\delta_r)\\
& +D_r(l_r\dot{\theta}\cos\theta - \dot{y})/E.
\end{aligned} \quad (5)
$$

$$
\begin{aligned}
I\ddot{\theta} =\ & l_f(F_f\sin\delta_f + U_f\cos\delta_f)\\
& -l_r(F_r\sin\delta_r + U_r\cos\delta_r)\\
& -l_r D_r(l_r\dot{\theta} + \dot{x}\sin\theta - \dot{y}\cos\theta)/E.
\end{aligned} \quad (6)
$$

Here,

$$E = \sqrt{\dot{x}^2 + \dot{y}^2 + l_r^2\dot{\theta}^2 + l_r\dot{x}\dot{\theta}\sin\theta - 2l_r\dot{y}\dot{\theta}\cos\theta}. \quad (7)$$

In this case, the cornering forces are regarded as a linear function of the slip angle and are written as follows:

$$
\begin{aligned}
U_f &= -2K_f\beta_f,\\
U_r &= -2K_r\beta_r
\end{aligned} \quad (8)
$$

where K_f and K_r are the cornering power of the front and rear tires, respectively. The lateral stability of this vehicle is calculated by using ydirectional motion and yaw rotation.
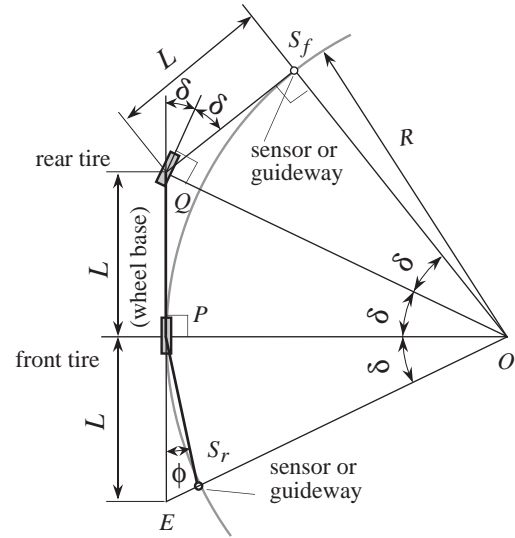
Fig. 1. Schematic representation of SSM
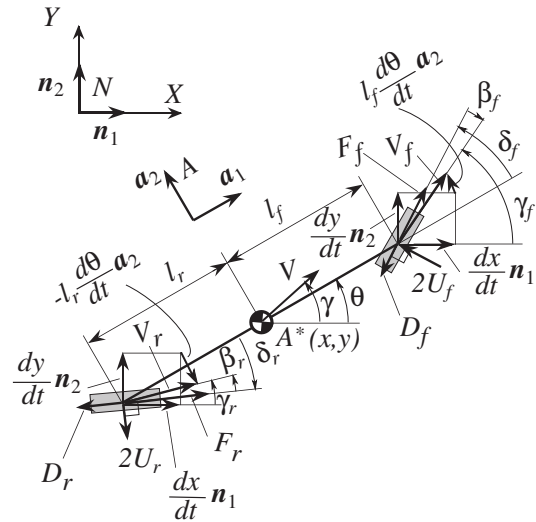
Fig. 2. Schematic diagram of a vehicle model

When $|\gamma|$ and $|\theta|$ are small value, then slip angles of the front and rear tires are.

$$
\begin{aligned}
\beta_f &= y + \frac{l_f\theta}{V} - \theta - \delta_f, \quad (9)\\
\beta_r &= y - \frac{l_r\theta}{V} - \theta + \delta_r.
\end{aligned}
$$

Substitute equation (8) to equation (5) and (6). The dynamical equation of motion by the body fixed coordinate is derived as follows;

$$\mathbf{M}\ddot{\mathbf{X}} + \mathbf{C}\dot{\mathbf{X}} + \mathbf{K}\mathbf{X} = \mathbf{F}\mathbf{u} \quad (10)$$

Here,

$$\mathbf{M} = \begin{bmatrix} m & 0\\ 0 & I \end{bmatrix},$$

$$\mathbf{C} = \frac{2}{V}\begin{bmatrix} K_f + K_r & l_f K_f - l_r K_r\\ l_f K_f - l_r K_r & l_f^2 K_f + l_r^2 K_r \end{bmatrix},$$

$$\mathbf{K} = \begin{bmatrix} 0 & -2(K_f + K_r)\\ 0 & -2(l_f K_f + l_r K_r) \end{bmatrix},$$

$$\mathbf{F} = \begin{bmatrix} 2K_f & -2K_r\\ 2l_f K_f & 2l_r K_r \end{bmatrix},$$
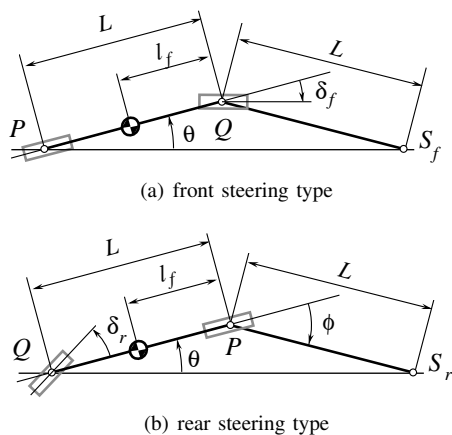
Fig. 3. Schematic of a vehicle driving on the straight path with SSM

$$\mathbf{X} = \left[\begin{array}{c} y \\ \theta \end{array} \right],$$

$$\mathbf{u} = \left[\begin{array}{c} \delta_f \\ \delta_r \end{array} \right].$$

III. STABILITY ANALYSIS

A. Feedback System by SSM on Straight Line

Figure 3 shows the geometrical relation moving on the straight line when the steering type vehicle are controlled by SSM. In this figure (a) and (b) show the front and rear steer type SSM, respectively. By using these figures the feedback control system following to the straight line is constructed. If the eigenvalues of a system matrix are calculated and stayed in left half plane, the constructed control system is the stable. The state variables are selected as follows;

$$\mathbf{x} = \left[\begin{array}{cccc} \dot{y} & \dot{\theta} & y & \theta \end{array} \right]^T \qquad (11)$$

and, the state equation is transformed from equation (9).

$$\dot{\mathbf{x}} = \mathbf{A}\mathbf{x} + \mathbf{b}u \qquad (12)$$

Here,

$$\mathbf{A} = \left[\begin{array}{cc} -\mathbf{M}^{-1}\mathbf{C} & -\mathbf{M}^{-1}\mathbf{K} \\ \mathbf{I} & \mathbf{0} \end{array} \right],$$

$$\mathbf{b} = \left[\begin{array}{c} \mathbf{M}^{-1}\mathbf{F} \\ \mathbf{0} \end{array} \right].$$

Feedback gain $\mathbf{G}$ of this system is derived by using Fig. 3 on each steering type.

$$u = -\mathbf{G}\mathbf{x} \qquad (13)$$

And a new system matrix included feedback by SSM is obtained as follows;

$$\mathbf{A} - \mathbf{b}\mathbf{G} \qquad (14)$$

Finally, a feedback gains of front steer type in Fig. 3(a) aer

$$\mathbf{G} = \left[\begin{array}{cccc} 0 & 0 & 0 & 1 \\ 0 & 0 & 0 & 0 \end{array} \right] \qquad (15)$$

And, a feedback gains of rear steer type in Fig. 3(b) are

$$\mathbf{G} = \left[\begin{array}{cccc} 0 & 0 & 0 & 0 \\ 0 & 0 & 0 & 4 \end{array} \right] \qquad (16)$$
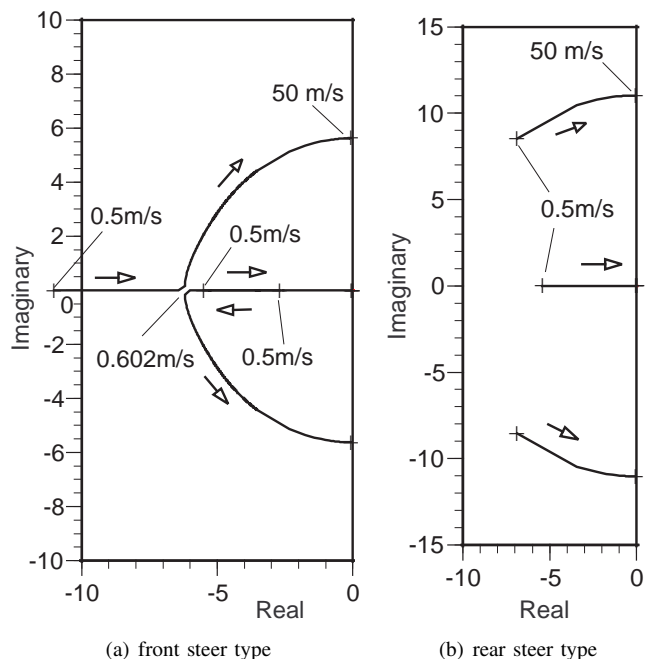
Fig. 4. Eigenvalue plot of SSM following by straight line
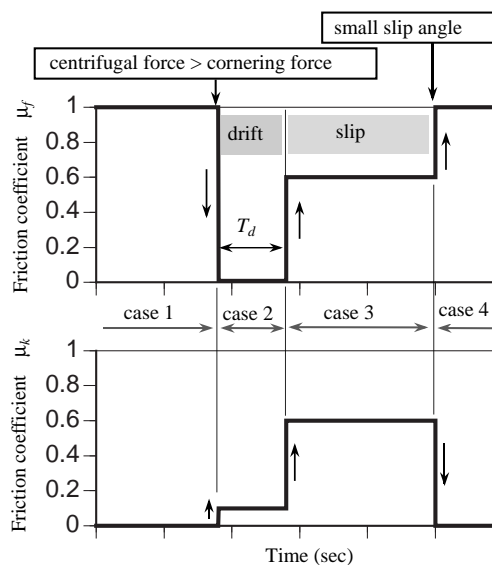
Fig. 5. Prediction of friction model

B. Calculation of Eigenvalues

Table 1 shows a rear steer type robotic vehicle developed in this paper. In order to compare with this type and a front steer type, this table also shows parameters of rear steer type when it moves backward. Figure 4 shows eigenvalues of equation (12) if the vehicle moves 0.5 to 50m/s on the straight line. Each plot shows that the front and rear steer type SSM are also stable. But the stability performance of rear steer type is worse than the front type one.

IV. SIMULATION RUNNING ON THE COURSE

A. Tire characteristics

In the previous paper, the relationship between the lateral force and the slip angle were measured using a test equipment. These data are also used in the present paper. Figure 3 shows the measured lateral forces generated by the tire when

the contact forces are set at 3.63N and 4.12N. These data are approximated to the fourth polynomial by using the least squares method as follows:

$$
\begin{aligned}
U_1^{static}(\beta) = \ & -2.146 \times 10^{-5}\beta^4 \\
& +1.824 \times 10^{-3}\beta^3 \\
& -5.923 \times 10^{-2}\beta^2 \\
& +0.958\beta + 8.391 \times 10^{-2} \quad (17)
\end{aligned}
$$

$$
\begin{aligned}
U_2^{static}(\beta) = \ & -2.542 \times 10^{-5}\beta^4 \\
& +2.183 \times 10^{-3}\beta^3 \\
& -7.066 \times 10^{-2}\beta^2 \\
& +1.118\beta + 5.146 \times 10^{-2} \quad (18)
\end{aligned}
$$

Equation (15) is equivalent to equation (16) multiplied by the contact force ratio 4.12/3.63. In this case the cornering force is proportionate to the contact force of the tires. For the simulation, twice the cornering force is applied to the body because the front and rear axles have two tires.

B. Variable kinetic friction model of tires

Coulomb friction is applied in the present paper, and a variable kinetic friction model, shown in Figure 4, is proposed for simulating the drifting cornering motion at high speed. Case 1 is a static friction condition, which does not involve slipping between the ground and the tires, and the cornering forces U_f and U_r are approximately equal to the values given by equations (5) and (6). Case 2 is a drifting condition, which involves slipping between the ground and the tires. While Case 2 involves two sets of forces, i.e., the friction force acting in the direction opposite to the speed vector of the tires and the cornering force, which is small because the moving direction of the vehicle is not changed by the steering angle. These sets of forces use the friction coefficient μ_k and the friction coefficient μ_f, respectively. For the transformation to the drifting condition (Case 2), the cornering force must be smaller than the centrifugal force of the body at high speed. The time for this period is T_d . Case 3 is also a slipping condition that involves sliding between the ground and the tires. The friction conditions were identical to those of Case 2, but not same values. This condition starts after time T_d of Case 2. Case 4 is identical to Case 1. When the slip angle becomes small, the condition begins to change from the slipping condition (Case 3) to the static friction condition (Case 4). When the front and rear wheels slide at the same time, posture control of the body becomes impossible. It is therefore assumed that only the rear tires enter the drifting condition (Case 2). The friction force D_r and cornering force U_r of the rear tires are as follows:

$$
D_r = W_r \mu_k \quad (19)
$$

$$
U_r = 2\mu_f U_r^{static}(\beta_r) \quad (20)
$$

where W_r and U_r static are the contact force and the cornering.

C. Simulation conditions

The course, which consists of two semicircles of radius 0.5m connected by straight segments of 0.7m in length, was used to analyze the turning motion, including drifting, of a laterally guided vehicle by the SSM. Dynamic analysis of the vehicle was performed by integrating equations (1) to (3) with the Runge-Kutta method. The calculation results for the center of gravity of the vehicle and the contact points of the guideway and the sensor were determined using the SSM. In addition, the calculated velocity vectors and the steering angles of the front and rear tires were used to determine the slip angles and cornering forces. For the simulation, physical parameters of rear steer type robotic vehicles shown in table 1. H is the height of the center of gravity form the road surface, b is the tread, W_f and W_r are the loads on the front and rear tires, respectively. In addition, the initialization parameters of the numerical values are shown in Table 2. The driving force can be obtained using the equation of motion by setting $F_f = 0$ for the vehicle. The supplied current of the DC motor is set to a constant value, the driving torque of the driven wheel is defined by the angular velocity and torque relations of the DC motor, as follows:

$$
F_{drive} = (N_f - 60V_{drive}\frac{n_d}{2\pi r_{tire}})\frac{T_m}{N_f}\frac{n_d}{r_{tire}} \quad (21)
$$

where F_{drive} is the driving force, N_f is the no-load speed of the motor, V_{drive} is the speed of the driving wheel, n_d is the gear ratio, rtire is the tire radius, and T_m is the stalling torque of the motor. Table 3 shows the parameters of the DC motor used for the simulation. Here, the tire radius r_{tire} and the gear ratio n_d are 0.0295m and 4.57, respectively. The cornering forces of this vehicles are

$$
U_f = 2U_1^{static}(\beta_f)\mu_s \quad (22)
$$

$$
U_r = 2U_2^{static}(\beta_r)\mu_f \quad (23)
$$

Here, μ_s is used to compensate the measured tire characteristic and the friction coefficient of the road surface. This value is given arbitrary in the simulation. In addition, the compensation parameter of rear tires is included in μ_f.

D. Simulation results

Simulations are started from the initial point and speed at 1.3m/s and 2.1m/s shown in Table 3. In the simulations the control delay of steering angle control system is set at 32ms by the measurement of experimental setup . Let the calculated trajectory close to the experimental results by changing friction parameters μ_s and μ_f. By the way, a simulation at the low speed about 1.3m/s is shown in Fig 6. In this case the drift condition is not appeared during moving because of slow-speed. Figure 6 and 7 show the simulated results of rear steer types of SSM with friction parameters shown in Table 2. In these figures, (a), (b), (c) and (d) show the moving trajectories, velocities of front and rear axle, steering angle and slip angles of front and rear tire, respectively. Figure 7 shows that a large steering angle makes at each entrance of the corner, the drift condition is generated for a moment by a large slip angle, and the moving speed of front and rear axles decrease while the rear axle is turning outside of the course. The trajectory of front axle is staying on the course and the vehicle has achieved a steady state running. Thus, the accurate simulation results gives us an information with effective characteristics of the controlled vehicle.
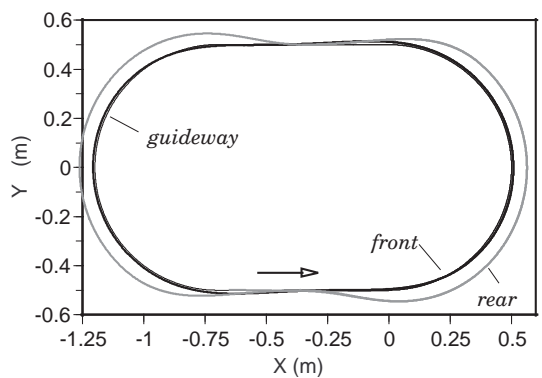
(a) loci
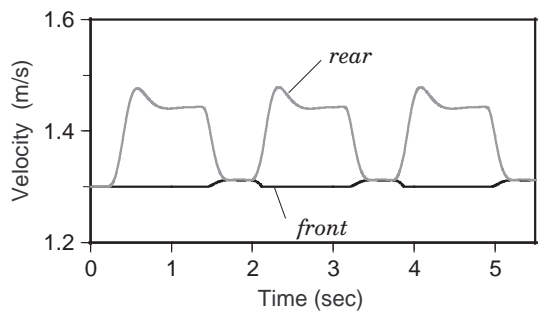
(b) velocity
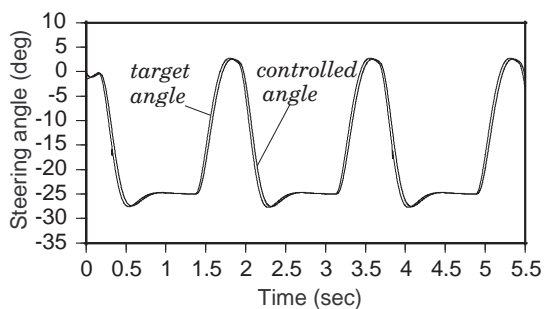
(c) steering angle
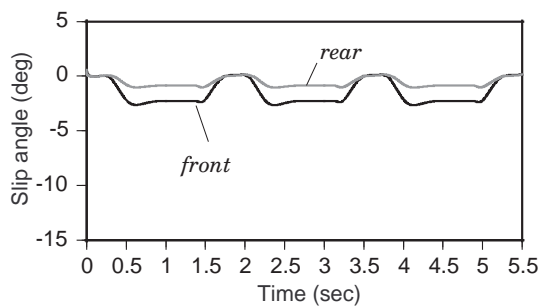
(d) slip angle

Fig. 6. Simulated result running on the path at slow-speed
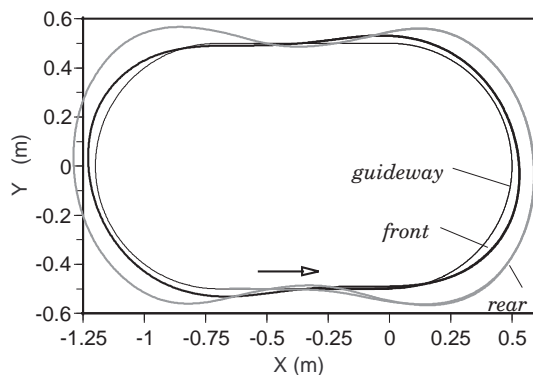
(a) loci
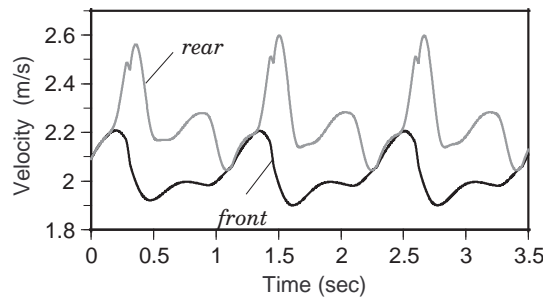
(b) velocity
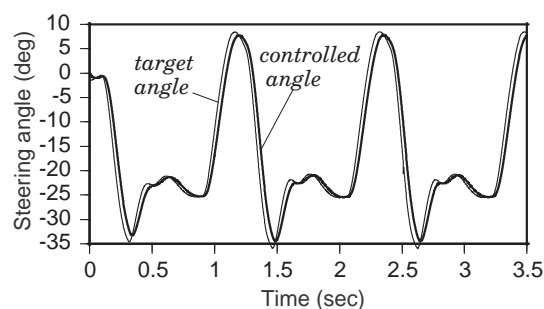
(c) steering angle
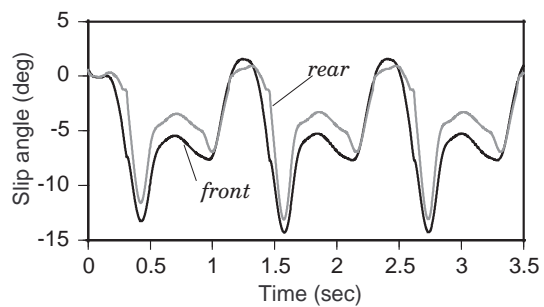
(d) slip angle

Fig. 7. Simulated result running on the path at high-speed

V. EXPERIMENTAL SETUP AND RESULTS

A. Rear Steer Type Robotic Vehicle with SSM

Figure 8 shows an outside view of rear steer type SSM robotic vehicle which is developed for the experiment. Figure 9 shows outline and dimension of this robot. The wheel base is 0.225m, the tread is 0.135m, and the gross weight is 1.4kg. Two reflective markers are pasted at the front and rear axle and measured the position by 3D measurement system. 1kHz CMOS camera located at the front axle follows a 0.02m white line pasted on black face course. The steering angle is controlled by two times of camera angle which is sensed by the rotary encoder. The lateral control of rear steer type vehicle is achieved consequently by SSM method. The physical parameters of this vehicle are the same as the simulation. The rotational angle of CMOS camera is controlled by servo motor through the deceleration gear. The rear steering angle is driven by the radio control servo motor of which original control circuit is replaced with the constructed controller. In order to get the perfect Ackerman geometry, a little improvement of the original body (made by TAMIYA INC.) was needed. The body is a monocoque structure made by a plastic. A double wishbone suspension

is adapted to the body, but the effect of suspension is not applied to the dynamical simulation. The vehicle is equipped with tread-patterned tender rubber tires, the insides of which were filled with sponge in order to produce soft contact with the load surface. The outside diameter and width of the tires were 0.059m and 0.023m, respectively. The data of the tire characteristics were measuredadn applied tothe simulation. The power source is used Ni-MH AAA type 10 cells (12 Volt) and installed inside of the body.

B. Control system

The construction of this controller is shown in Fig. 10. The robot control system is constructed with a H8S/2258F one-chip microcomputer (Renesas Technology) and is installed at the rear of the vehicle. The 1kHz intelligent camera captures an 8-bit image with 128×128 pixels every one millisecond. The sensor chip has 8 bit AD converters and charge amplifiers for each raw column, and can convert 128 pixels in one line at the same time. An image of one frame can be taken out by repeating this operation 128 times. The size of this CMOS image sensor is 7.4×11.2mm. 1kHz frame rate is archived by FPGA (Field Programmable Gate Array). Programming language of FPGA is written by verilog HDL. FPGA is programmed so that the microprocessor may access the image data like the memory of the bus connection.

C. Experimental conditions

For the experiment, a test track was built having a 0.02m wide strip of white tape on a black road surface. The geometry of the test track was identical to that used in the simulation conditions. The surface material was constructed using acrylic film. Comparison of the simulated and experimental results required measurement of the locus of the actual robot. Experimental data were acquired using a ProReflex(QUALISYS) three-dimensional motion capture system having a sampling rate of 240 times per second and a measuring error of within ± 0.2 mm. This measurement system captures the threedimensional position of two reflecting makers attached to centers of the front and rear axles, and the captured data is output to a text file. A constant pulse width is applied to a motor driving circuit that produces a constant driving force condition equivalent to the simulation conditions. In this experiment, the maximum speed of the vehicles was set to 2.2m/sec. In the experiment, the control program stores the steering angle and the controlled variable in the built in RAM every 2 ms. After the run, the data is uploaded to a personal computer.

D. Experimental results

Figure 11 and 12 show an experimental data running on the test course when the vehicle is moving at low-speed and high-speed. In these figures (a) is the trajectory of front and rear axle, (b) is the moving speed of front and rear axle, (c) and (d) are the steering angle and the difference of target value and measured value uploaded by the robot controller, respectively. At the low-speed moving the front axle passes on the guideway and the rear axle moves outside of circle according to the geometrical relation shown in Fig. 1. Figure 11(a) shows that the speed of rear axle is faster
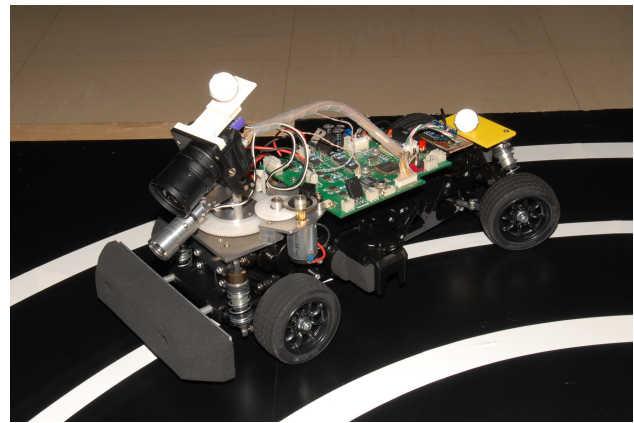
Fig. 8.   Outside view of developed SSM robot vehicle
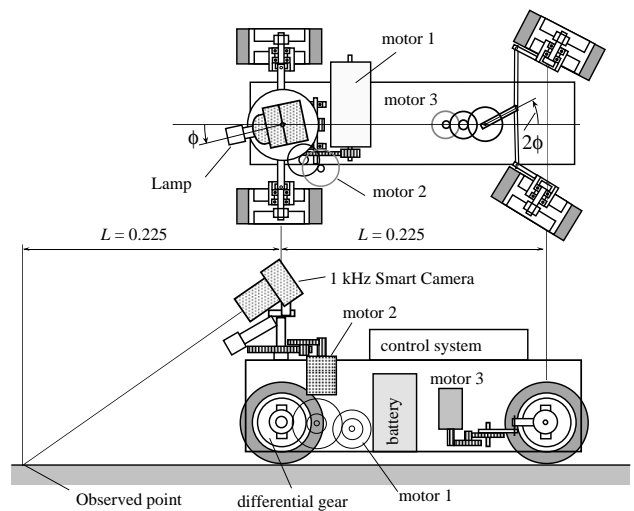
Fig. 9.   Outline of constructed rear wheel steer vehicle
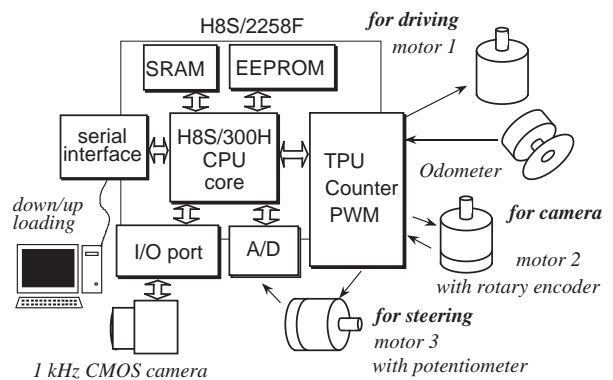
Fig. 10.   Control system for rear wheel steer SSM

than front axle because the rear axle moves the outside of the circle at the corner. I seems that the front part of robot vehicle is moving at almost same speed. The control effect of SSM is confirmed by the experiment. The interesting results are obtained from the high-speed moving experiment. In Fig. 12(a) the front axle appears the tracking error when the vehicle is passing through outside of the guideway at the corner. At the same time the rear axle is moving a long way off the guideway. But the robot vehicle keeps the steady state running on the course. By comparing with Fig. 7 and 12, the simulation result is well corresponding
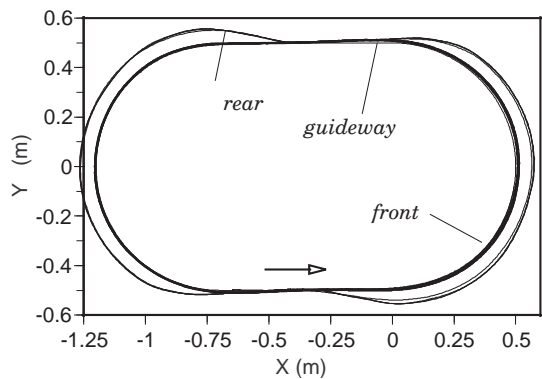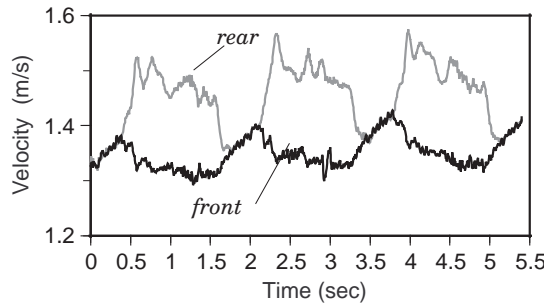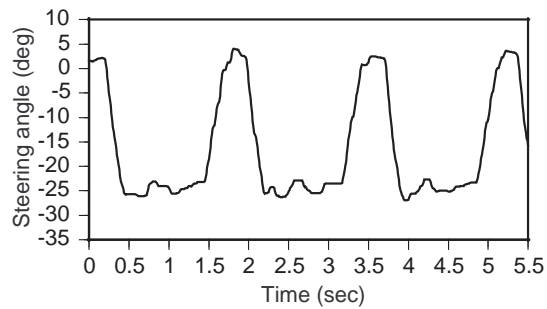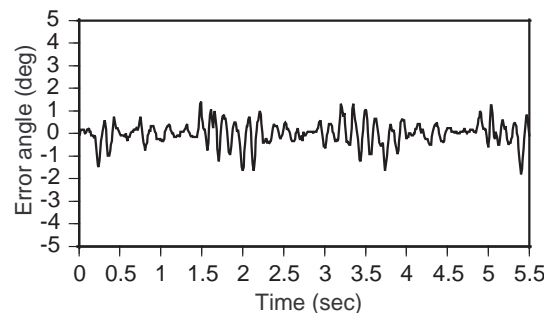
Fig. 11.   Experimental data running on the path at low-speed
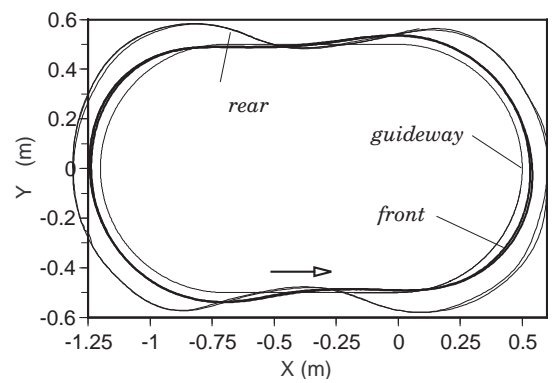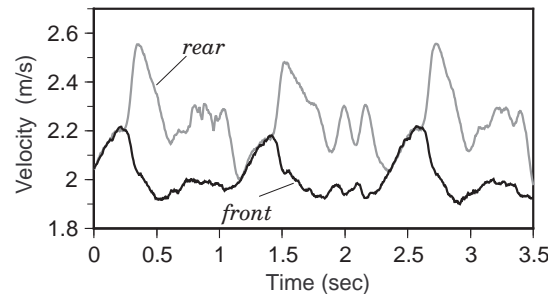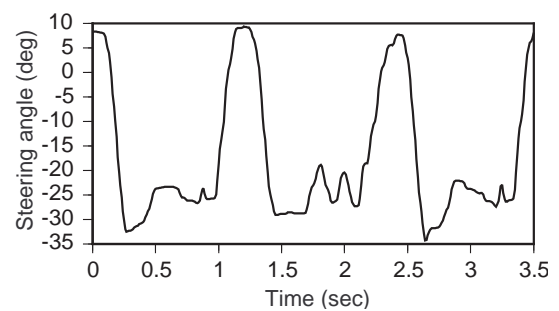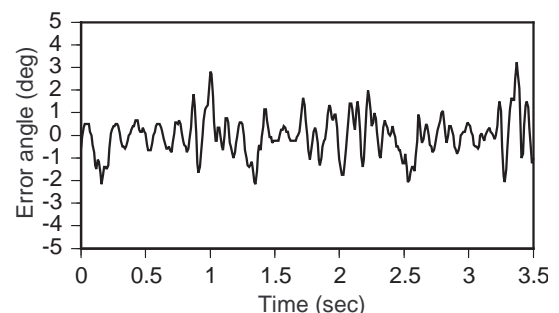
Fig. 12.   Experimental data running on the path at high-speed

with the high-speed moving experiment. Also the low-speed simulation Fig. 6 is well corresponding with the experiment Fig. 11. The drift condition at the entrance of the corner was necessary to match the moving track to the experimental results. According to the simulated result the rear tires are steered radically at the entrance of corner, then rear tires slip for a little while and passes far away from the guideway after the contact force is recovered. Figure 11(d) and 12(d) show the errors of the steering angle and target value given by the camera angle. By the comparing with Fig. 11(d) and 12(d), a major cause for the error is the delay of control system.

Although SSM achieved a steady state running on the test course at high-speed.

VI. CONCLUSION

This paper proposed SSM which is a lateral guided method for rear steer vehicle. The idea of SSM is that the sensor is located at the tip of the sensor arm of which length is the same as the wheel base of vehicle, and the steering angle is two times of sensor arm angle on opposite direction. This relation is obtained by the linear approximation. In this paper a SSM robotic vehicle is developed and the dynamical model

of rear steer vehicle is derived and calculated. The experimental and simulated results are shown that SSM achieves the steady state tracking even if the drift condition is occurred at the entrance of corner. Experiment and simulation results are well correspond with each other. Finally, advantages of SSM are that system is a simple and the stable behavior is obtaied. And SSMs are able to use for not only the front steering vehicle and reverse phase four-wheel steering but also the rear steering type.

REFERENCES

[1] Abe, M., Vehicle Dynamics and Control, (1979), kyoritsu Publication(in Japanese),pp.192-213.
[2] Minami, M., et al., Magnetic Autonomous Guidance by Intelligent Compensation System, Vol.31, No.5(1987),pp.382-391..
[3] Makino, T., et al., High-Speed Driving Control of an Automatic Guided Vehicle Using an Image Sensor, Transactions of the Society of Instrument and Control Engineers, Vol.28, No.5(1992), pp.595-603.
[4] Shladover, S.E., et al., Steering Controller Design For Automated Guideway Transit Vehicles, Transactions of the American Society of Mechanical Engineers, Vol. 100, (1978), 1-8
[5] Tsunashima, H., A Simulation Study on Performance of Lateral Guidance System for Dual Mode Truck, Transactions of the Japan Society of Mechanical Engineers, Series C, Vol.65, No.634(1999), pp.2279-2286.
[6] http://www.grandchallenge.org/
[7] Takita, Y., High-speed Driving of a Lateral Guided Vehicle with Sensor Steering Mechanism, Transactions of the Japan Society of Mechanical Engineers, Series C, Vol.65, No.630(1999), pp.622-629.
[8] Takita, Y., et al., High-speed Cornering of Lateral Guided Vehicle with Sensor Steering Mechanism, Transactions of the Japan Society of Mechanical Engineers, Series C, Vol.66, No.652(2000), pp.3888-3896.
[9] Takita, Y., Drift Turning of Lateral Guided Vehicle with Sensor Steering Mechanism(Application of a Variable Kinetic Friction Model), Transactions of the Japan Society of Mechanical Engineers, Series C, Vol.68, No.675(2002), pp.3170-3177.
[10] Takita, Y., Sakai, Mukouzaka, N. and Date, H., Control of Lateral Guided Vehicle with Sensor Steering Mechanism Using Miniaturized 1kHz Smart Camera(Stabilization by Dynamic Damper), Transactions of the Japan Society of Mechanical Engineers, Series C, Vol.71, No.701(2005), pp.193-199.
[11] Takita, Y., Sakai, Y., Takahashi, T., Date, H. and Mukouzaka, N., Increasing the Speed of a Lateral Guided Vehicle with a Sensor Steering Mechanism Using 1kHz Intelligent Camera (Drift Control by Changing of Steering and Arm Length Ratio), Transactions of the Japan Society of Mechanical Engineers, Series C, Vol.72, No.717(2006), pp.1558-1565.
[12] Takita, Y., Date, H. and Ohkawa, S., Dynamical Characteristics of a Lateral Guided Robotic Vehicle with a Rear Wheel Steering Mechanism Controlled by SSM, Proceedings of the World Congress on Engineering and Computer Science 2011, WCECS 2011, 19-21 October, 2011, San Francisco, USA, pp.306-311.

TABLE I
PARAMETER OF ROBOTIC VEHICLE

	front steerer type		rear steerer type	
I	0.0058	kgm^2	0.0058	kgm^2
l_f	0.075	m	0.15	m
l_r	0.15	m	0.075	m
L	0.225	m	0.225	m
m	1.378	kg	1.378	kg
K_f	0.5929	N/rad	1.2238	N/rad
K_r	1.2238	N/rad	0.5929	N/rad

TABLE II
PARAMETERS OF VEHICLE

I	5.8×10^3	kgm^2	W_f	9.02	N
m	1.378	kg	W_r	4.49	N
b	0.134	m	l_f	0.075	m
L	0.225	m	l_r	0.15	m
H	0.050	m			

TABLE III
INITIAL VALUES FOR SIMULATION

	Slow-speed	High-speed
V	1.3 m/s	2.1 m/s
A(x,y)	(-0.5m,-0.5m)	(-0.5m,-0.5m)
θ	0.0rad	0.0rad

TABLE IV
ESTIMATED FRICTION PARAMETER

	case 1	case 2 (drift)	case 2(slip)
μ_s	0.9	0.72	0.72
μ_f	1	0.01	0.54
μ_k	0	0.01	0.81
T_d	-	0.018 sec	